Self-Diffusion and Probe Diffusion in Dilute and Semidilute Aqueous Solutions of Dextran

Ruth Furukawa,† José Luis Arauz-Lara,‡ and Bennie R. Ware*

Department of Chemistry, Syracuse University, Syracuse, New York 13244-4100

Received December 27, 1989; Revised Manuscript Received June 29, 1990

ABSTRACT: Tracer diffusion processes in polymeric solutions of dextran in both the dilute and semidilute regimes were investigated by the fluorescence photobleaching recovery technique. The molecular weight of the matrices covered the range from 40 kDa to 2 MDa. The tracer species consisted of fluorescein-labeled dextrans of molecular weights 40 and 150 kD, fluorescein-labeled polystyrene spheres of 38-nm diameter, and fluorescein (molecular weight of 332 Da). The viscosity of selected solutions was measured with capillary viscosimeters. We report here an extensive set of experimental data on diffusion processes and viscosity, obtained from a consistent set of samples. Comparison of our data with some of the current models is presented.

Introduction

Transport mechanisms in polymer solutions and melts have been the object of increasing attention over the past 2 decades. Particular emphasis has been placed on an attempt to understand the mechanisms for diffusion through polymer solutions whose concentrations are sufficiently high that intermacromolecular interactions must be considered. For the diffusion of linear polymers in highly entangled systems such as concentrated polymer melts, cross-linked gels, and concentrated solutions of high molecular weight polymers, the reptation mechanism modeled by de Gennes[1,2] appears to be quite successful. The reptation model predictions that the translational diffusion coefficient D should scale with the molecular weight of the diffusing species as M^{-2} and with the concentration of the entangled matrix as $c^{-1.75}$ in good solvents and c^{-3} in Θ solvents appears to be confirmed, though the prediction that the shear viscosity should vary as M^3 is somewhat at variance with the established $M^{3.4}$ dependence.

Scaling theory employing the reptation concept has also been used to model the intermediate or semidilute regime.[2] Definition of an appropriate model for this regime, however, is more complicated than for either the dilute or concentrated solution limits. The semidilute regime is essentially a transition zone. The transition from dilute to semidilute behavior is predicted to occur at the concentration c^* for which polymer domains must overlap. Estimations of c^* may vary by as much as a factor of 2 or 3, and the onset of the reptation mechanism must be seen realistically as a gradual transition as the number of entanglements increases. Additional complications that arise throughout the semidilute regime include the effect of polymer concentration on the monomer friction factor, the effect of polymer concentration on the effective solvent quality, the dynamic nature of the constraints from the reptation "tube" presented by surrounding polymers, and the effect of the motion of each polymer on the mobilities of the polymer molecules that form its reptation tube.[3]

Both the theoretical interest in diffusion in the semidilute regime and the recognized practical importance of understanding this problem have prompted a large number of experimental investigations designed to test the predicted scaling relationships. This work has been made possible by the development of several modern techniques for the study of translational diffusion, particularly dynamic light scattering (DLS), forced Rayleigh scattering (FRS), pulsed-field-gradient nuclear magnetic resonance (PFGNMR), and fluorescence photobleaching recovery (FPR). Comprehensive reviews are available for historical perspective.[3,4] We will attempt to summarize the current issues with selected citations from the recent literature.

Although an early study of polystyrene self-diffusion in benzene by Leger et al.[5] confirmed that $D \propto M^{-2}c^{-1.75}$, subsequent reports have emphasized the deviation of experimental data from the scaling prediction. The M^{-2} behavior has been confirmed in one report,[6] but significant deviations from this behavior have also been reported.[7-9] Kim et al.[8] used mixed polymer solutions to investigate the effect of matrix molecular weight P. They found that the probe chain does not reach its large-P limit until P is 3–5 times M, suggesting that pure reptation, which predicts that D is independent of P, does not apply to self-diffusion. The dependence of D on concentration is not well expressed by a simple power. The predicted behavior $D \propto c^{-1.75}$ is often observed over a narrow concentration range, but studies over wide ranges of concentration show a continuously varying exponent, often tending toward the predicted limit of $D \propto c^{-3}$ at high concentrations.[7-9] Wesson et al.[6] also tested the prediction of Graessley,[10] based on the Doi–Edwards model,[11] that $D_s \propto \eta_0^{-1}c^2$, where η_0 is the viscosity of the solution, and did not find agreement. They did find good agreement with the Rouse theory prediction that $D_s \propto \eta_0^{-1}c$.

Lodge and Markland[12] compared the diffusion of 12-arm star polystyrenes with linear polystyrenes over a range of concentrations and have found their behavior to be remarkably similar. Since the star-branched polymer cannot reptate, the conclusion was drawn convincingly that reptation is also not an important mechanism for the linear polymer. However, a subsequent paper from the same group[12a] produced extensive data in support of the opposite conclusion. Shull et al.[13] found that three-, four-, and eight-arm stars diffused with about equal facility in microgel matrices. They attributed their observation to an arm retraction mechanism. Phillies[14] contends that the diffusion of spherical probes and of linear polymers follows the same empirical behavior and thus that reptation is not an important mechanism for the latter. The diffusion of a spherical probe through an entangled

* To whom correspondence should be addressed.
† Present address: Department of Zoology, University of Georgia, Athens, GA 30602.
‡ Present address: Departamento de Fisica, CINVESTAV IPN, Apto. Postal 14-740, 07000 Mexico D.F., Mexico.

0024-9297/91/2224-0599$02.50/0

network of polymers is generally found to obey the relationship

$$D/D_0 = \exp[-\alpha c^{\nu}] \quad (1)$$

where D_0 is the diffusion coefficient of the probe in pure solvent, c is the concentration of the matrix polymer, and α and ν are scaling parameters. Equation 1 can be argued from several theoretical perspectives;[15-17] it has been verified by numerous experimental examinations (surveyed in ref 14; more recent studies include refs 18–20.) The principal objections to eq 1 have been the lack of consistency of the parameters α and ν among different data sets and the absence of physical significance for these parameters.[12,18,19] Phillies[17] has presented a heuristic derivation of eq 1 that permits molecular interpretations of α and ν, but the spread in available experimental data prohibits credible validation.

We report here an extensive set of measurements on the diffusion of dextrran molecules in solutions of dextran, on the diffusion of polystyrene spheres in solutions of dextran, and on the diffusion of a much smaller molecule (fluorescein) in these same solutions. The matrix dextran concentration has been varied through the dilute and semidilute concentration regimes; several molecular weights have been employed. Measurements have been made by using the technique of fluorescence photobleaching recovery (FPR), which provides a determination of the tracer diffusion coefficient of a fluorescent species. In addition, we have determined the macroscopic viscosity of a selected set of solutions. The motivation for these measurements is to provide a data set characterizing polymer diffusion, self-diffusion, probe diffusion, microscopic viscosity, and macroscopic viscosity on a consistent set of samples using the same techniques so that a systematic comparison can be made with the present theories and with ideas that may evolve in the future.

Experimental Methods

A. Materials. Fluorescein-labeled dextrans of molecular weights 40.5 kDa (lot 54F-0593) and 150 kDa (lot 14F-0152) were obtained from Sigma. The dextrans were exhaustively dialyzed against distilled, deionized water to remove free fluorescein and then against 200 mM potassium phosphate buffer at pH 8. Each solution was prepared just prior to use. Fluorescein-labeled polystyrene latex spheres (PSLS) of diameter 38 nm were obtained and treated as described previously.[29] The suspension of spheres was subjected to ultrasonication and centrifugation to remove aggregates just prior to use. The final concentration of spheres in the dextran solutions was 0.56 g/L, which is a volume fraction of approximately 5.3×10^{-4}.

Dextrans of 40.6 kDa (lot 114F-0335), 83 kDa (lot 54C-0326), 500 kDa (lot 96C-0402), and 2.0 MDa (lot 18C-0184) were obtained from Sigma. A dextran of molecular weight of 110 kDa (245919-1084) was obtained from Fluka, A.G. The dilute dextran solutions (<100 g/L) were prepared by dissolution in distilled, deionized water, stirred 24 h, and diluted with phosphate buffer to the final concentrations. Concentrated dextran solutions (>100 g/L) were prepared by allowing the polymer to swell 3 days in 200 mM phosphate buffer and then stirred for 3 days. All concentrations were checked by drying the stock solutions to a constant weight.

B. Viscometry. Viscosity measurements were made with either a semimicro or micro Cannon Ubbelohde viscometer calibrated by the manufacturer (Cannon Instrument Co., State College, PA). The flow times were sufficiently long so that kinetic energy corrections were negligible and subsequently ignored. Kinematic viscosities were converted to viscosities by use of the density data reported in ref 21 and the buffer density

$$\rho = 1.024 + 3.76 \times 10^{-4} c \quad (2)$$

where c is in g/L.

C. Fluorescence Photobleaching Recovery (FPR). Tracer diffusion coefficients were determined by the method of fluorescence photobleaching recovery (FPR).[22-25] In this method the diffusion of a fluorescent probe is observed by photochemically bleaching a pattern within the sample and measuring the characteristic time for the dissipation of the created pattern. Our measurements were made by the modulation detection method[26] developed in our laboratory and applied to probe diffusion studies previously.[27-29] To summarize this method briefly, a sample containing fluorescent probes is loaded into a microcuvette, which is then placed on the stage of a fluorescence microscope. A periodic square wave pattern is irreversibly photobleached into the sample by a brief, intense laser pulse through a grating, which is placed at the rear focal plane of the microscope. The grating is then translated at a constant velocity through the attenuated reference beam to produce a moving pattern on the specimen. A modulation of fluorescence emission is produced as the bleached pattern and the moving illumination fall into and out of phase. The photocurrent generated thus contains an ac component whose frequency is determined by the spacing and velocity of the grating and whose amplitude relative to the dc component is determined by the extent of photobleaching. In effect, the modulation ac envelope $E(t)$ is a measure of the spatial Fourier component of the fluorescence intensity with wave vector K' given by

$$K' = 2\pi/L \quad (3)$$

where L is the period of the pattern formed by the projection of the grating at the specimen. For a species undergoing random translational diffusion with a single characteristic diffusion coefficient D, the modulation envelope decays exponentially according to the equation

$$E(t) = E(0)e^{-DK'^2 t} \quad (4)$$

All of the data in this study were fit well by eq 4.

The experiment wave vector K' was selected by variation of the magnifying power of the objective that focused the pattern onto the microscope stage. The value of K' was varied according to the size of the probe particle being studied and the concentration of the dextran matrix in order to arrange for the relaxation times to fall into an experimentally convenient time range. For experiments utilizing PSS as the probe $K' = 2127$ cm^{-1}, for fluorescein $K' = 333$ cm^{-1}, for the FITC dextran $K' = 841$ cm^{-1}, and at high dextran concentration $K' = 2127$ cm^{-1}. All diffusion and viscosity measurements were performed at 25 °C.

Results and Discussion

The primary data of this report are a large number of tracer diffusion coefficients of fluorescein, fluorescein-labeled dextrans, and polystyrene spheres in dextran matrix polymers of several different molecular weights over a range of concentration of each matrix polymer, plus the macroscopic viscosities of selected solutions. For the benefit of other workers in this field who may wish to investigate alternative schemes of analysis, we have tabulated these data (Tables S1–S5) and made them available as supplementary material (described at the end of this article). The data will be presented here in graphic and parameterized form to illustrate the hypotheses tested and the conclusions drawn in our analysis.

The infinite-dilution values, D_0, for the tracer diffusion coefficients of the open-chain probe molecules were measured to be 64×10^{-7} cm^2 s^{-1} for fluorescein, 5.1×10^{-7} cm^2 s^{-1} for 40-kDa dextran, and 2.7×10^{-7} cm^2 s^{-1} for 150-kDa dextran. These values obey the simple power law $D_0 \propto M^{-x}$, where M is the molecular weight of the probe molecules. From our values the exponent is determined to be $x = 0.52$, very near the value (0.57) determined previously for dextran in water[30] and consistent with the model of a linear Gaussian chain with some excluded volume.

At finite matrix mass concentration (c) the probe particles interact with those of the matrix. As a result of

those interactions the tracer diffusion coefficient of the probe is diminished from its D_0 value. In the dilute regime the only interactions between the probe and the host polymers are the excluded volume and the hydrodynamic interactions. The former are direct interactions due to the impossibility for a given particle to penetrate the physical space occupied by other particles in the system, and the latter are indirect interactions mediated by the solvent arising due to the motion of the particles. In this regime of low concentrations, the friction constant may be represented as a power series expansion in the concentration. It has been observed previously[30,31] that the linear term is sufficient to describe the friction coefficient concentration almost up to c^*. We have therefore fit these data to an equation of the form

$$D = D_0(1 - kc) \tag{5}$$

Figure 1 shows fits of the data for the dilute regime to eq 5 for the two cases that most closely approximate self-diffusion: 40-kDa-labeled dextran in 40-kDa dextran, and 150-kDa-labeled dextran in 110-kDa dextran. The values of k determined from Figure 1 will be used subsequently to estimate values for c^*. Table I presents the values of k determined for the diffusion of fluorescein, 40-kDa dextran, and 150-kDa dextran in dextran matrices of different molecular weight. All data sets were found to have a linear regime, with the concentration at which curvature began being lower for the highest molecular weight matrix. The general trend is for k to be weakly dependent on both the probe molecular weight and the matrix molecular weight, except that fluorescein diffusion is not sensitive to matrix molecular weight, in agreement with a recent report from other investigators.[32]

The vast experimental evidence about tracer diffusion in polymeric solutions shows that this phenomenon does not exhibit any abrupt change around c^*. Therefore one cannot use tracer diffusion measurements to determine c^* directly. The reported values for c^* are based either on the measurements of a characteristic length of the polymer, or on empirical relations between c^* and M, or on the comparison of the experimental data for D with theoretical predictions. We now propose an alternative method to estimate c^* that is based on the measurements of tracer diffusion in the dilute regime. From studies of tracer diffusion in dilute suspensions of colloidal particles, it is known that for particles interacting only through the excluded volume and hydrodynamic interactions, the tracer diffusion coefficient satisfies a linear equation[33]

$$D = D_0(1 - b\Phi) \tag{6}$$

where Φ is the volume fraction occupied by the colloidal particles. For ideal hard spheres

$$\Phi = 4\pi nR^3/3 \tag{7}$$

R being the physical radius of the spheres and n the particle concentration. In the linear regime we may be justified in equating the two final terms in eqs 5 and 6 to obtain

$$kc = b\Phi \tag{8}$$

Inserting eq 7 in eq 8 and substituting

$$c^* = 3M/4\pi N_A R^3 \tag{9}$$

where N_A is Avogadro's number, we obtain $k = b/c^*$. Both theory and experiment show[34,35] that the value of b is close to 2. Hence we suggest the approximation

$$c^* \cong 2/k \tag{10}$$

Using the values of k determined in our experiments

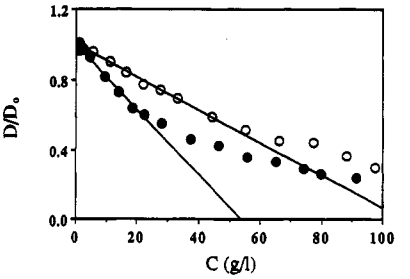

Figure 1. Plot of D/D_0 for dextran probes as a function of the total concentration of the probe and matrix dextran. The lines drawn are fits to eq 5. The lower line corresponds to the diffusion of 150-kDa-labeled dextran in 110-kDa matrix dextran (k = 0.0186 L g^{-1}); the upper line corresponds to the diffusion of 40-kDa-labeled dextran in 40-kDa dextran matrix (k = 0.00935 L g^{-1}).

(Figure 1), we calculate that c^* = 214 g/L for the 40-kDa dextran and c^* = 107 g/L for the 150-kDa dextran.

The molecular radius may be approximated by the hydrodynamic radius calculated by the Stokes–Einstein equation from the measured D_0 values

$$R_h = \frac{kT}{6\pi\eta D_0} \tag{11}$$

The values for R_h then are 4.4 nm for the 40-kDa dextran and 8.4 nm for the 150-kDa dextran. Calculation of c^* with eq 9 gives 186 g/L for the 40-kDa dextran and 100 g/L for the 150-kDa dextran, in reasonable agreement with our previous analysis. The lower values in this latter analysis may be attributable to the fact that the dilute-solution R_h is expected to be greater than the effective molecular radius in the semidilute regime. These values may also be compared with the c^* of ~12 wt % determined by Callaghan and Pinder[30] for 170-kDa dextran using PFGNMR and with a c^* of 80 g/L for 110 kDa dextran that may be obtained from the product of the reciprocal of the intrinsic viscosity[36] and the Einstein–Simha factor of 2.5.

In order to examine the dependence of the tracer diffusion coefficient on the molecular weight of the probe polymer and the molecular weight and concentration of the matrix polymer, we show a summary plot of log (DM^2) vs log c in Figure 2. The upper points are data for the 150-kDa dextran probe, and the lower set of points represents data for the 40-kDa dextran probe. Different symbols designate matrix molecular weights. The scaling rule of $D \propto M^2c^{-1.75}$ predicts that these points should fall on the same line of slope −1.75 in the semidilute regime above c^*. As expected, the downward curvature begins sooner for the 150-kDa probe (since c^* is lower), and for both probes the curvature begins well before the values of c^* we have calculated (log c^* = 2.33 for 40-kDa dextran; log c^* = 2.03 for 150-kDa dextran). For both probe polymers the slope of −1.75 is a reasonable fit through the region just above c^*. However, the slope decreases continuously with only a slight plateau. At the highest concentrations the slope approaches −3.0, the reptation theory prediction for Θ solvents. It is clear that in the semidilute regime at which the slope is −1.75, the molecular weight dependence is less than M^2, and the two sets of points do not coincide even at the highest concentrations attained, although clearly they are approaching each other. Close examination of the dependence of the tracer diffusion coefficient on the molecular weight of the matrix indicates a slight trend for matrices of higher molecular weight to be more effective at impeding diffusion; this effect is most pronounced for the highest molecular weight matrix and the highest molecular weight probe. Plots (not shown) of the reduced tracer diffusion coefficient D/D_0 versus matrix

Table I
Slope and "Infinite"-Dilution Value k and D_0, Respectively, of the Tracer Diffusion Coefficient of Different Probe Particles Obtained by Fitting Their Initial Decay to a Straight Line (See Eq 15)[a]

	fluorescein		40-kDa dextran		150-kDa dextran	
matrix M_w	$D_0 \times 10^6$	$k \times 10^2$	$D_0 \times 10^7$	$k \times 10^2$	$D_0 \times 10^7$	$k \times 10^2$
40.6 kDa	6.42	0.5	5.16	0.94	2.76	1.03
83 kDa			5.1	1.09	2.74	1.33
110 kDa			5.14	1.04	2.81	1.86
500 kDa			5.06	1.08	2.75	1.41
2 MDa	6.54	0.49	5.01	1.58	2.74	2.72

[a] D_0 is given in cm^2/s and k in L/g.

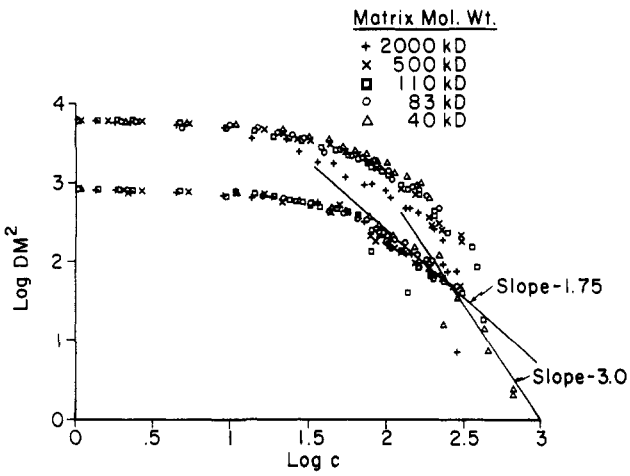

Figure 2. Plot of log (DM^2) vs log c, where D and M are, respectively, the diffusion coefficient and molecular weight of the probe dextran and c is the concentration of the matrix dextran. The legend in the figure indicates the symbols that designate different molecular weights. The upper points are data for the 150-kDa dextran probe, and the lower points are data for the 40-kDa dextran probe. As discussed in the text, this figure indicates that the scaling prediction for the concentration exponent (−1.75) is verified over a limited concentration range, but the M^2 behavior is not observed in this same range.

molecular weight at a fixed matrix weight concentration of approximately c^* for the 40-kDa dextran indicated a weak dependence above P = 500 kDa but a significant inverse relationship between P = 40 kDa and P = 500 kDa.

As discussed previously, the stretched exponential function (eq 1) has been shown to fit tracer diffusion data over a wide range of concentration. Phillies[17] has presented the first derivation of eq 1 to apply to the diffusion of a linear polymer probe in a matrix of linear polymers. His derivation is based on the assumption that the low-concentration hydrodynamic interactions induce self-similar effects on D when c is incremented infinitesimally. Starting from a low-concentration equation for D (eq 5), he obtained an expression similar to eq 1 from hydrodynamic effects alone. However, the original equation can be recovered only is ν = 1. Nevertheless, the Phillies derivation provides predictions for the scaling behavior of α, which scales as the geometric mean of the polymer molecular weights

$$\alpha \propto (MP)^{1/2} \tag{12}$$

and for ν, which is predicted to be 0.5 at high probe molecular weights, to be 1.0 at low probe molecular weights, and to scale as

$$\nu \propto M^{-1/4} \tag{13}$$

over an intermediate range of about 100–500 kDa (misprinted in the original article). Interpretation of stretched-exponential scaling parameters for other hydrodynamic observables has also been discussed in a recent article.[37]

In Table II are reported the values for α and ν, obtained by fitting our experimental values to eq 1, and in Figure 3 is shown the plot of α vs $(MP)^{1/2}$. From this figure one could say that for dextran α follows the behavior predicted by eq 12. Nevertheless, a closer examination of the values given in Table II shows that although for 150-kDa dextran α increases with P in a manner consistent with eq 12, the data for 40-kDa dextran do not exhibit any perceptible dependence on P. Concerning the values of ν, we can point out three observations: (1) They are, as most of the values reported in the literature, within the range 0.5–1.0. (2) While for 40-kDa dextran ν is independent of P (i.e., it is narrowly distributed around 0.925 (within 5%), for 150-kDa dextran it is not independent of P as predicted by eq 12. (3) There is a strong correlation between α and ν. Whether this correlation is only an artifact of the fitting procedure or it contains physical meaning is not clear. We have not included the error estimates (generally 5–10% rmse) from the fitting procedures for the parameters in Table II, because we believe they are underestimates. Reproducibility estimates from independent experiments have generally indicated standard deviations of about 15%.

A more physical view of spherical probe diffusion in a semidilute polymer solution was suggested by de Gennes and co-workers and communicated by Langevin and Rondelez.[15] These workers visualize the polymer matrix as a network with characteristic correlation length $\xi(c)$. The increased friction seen by a spherical probe of radius R is then predicted to be

$$f_0/f = \exp[-(R/\xi)^\delta] + \eta_0/\eta_m \tag{14}$$

where η_m is the macroscopic viscosity and η_0 is the solvent viscosity. The exponent δ is expected to be 2.5 for a gel with fixed entanglement points, 2.0 for ideal entangled chains, and less than 2 for real systems in which entanglement constraints are not rigid. The theory of Cukier[38] may be used to argue that δ = 1.0 in systems dominated by hydrodynamic screening. Since ξ is expected to scale as $c^{-3/4}$, the prediction has been made and recently confirmed[18] that a plot of log [log $[D_0/D]$] versus log c should have a slope of 0.75. Note, however, that this prediction ignores the concentration dependence of η_m. We have attempted to fit our probe diffusion data for spherical probes in dextran solutions to this same relationship and have found that there is a linear regime above a c of about 15 g/L, but the slope is higher than the predicted value, ranging from 0.85 to 1.09 for the different matrix molecular weights, with no clear trend in P dependence. In Figure 4 we show a plot designed to test eq 14 with the inclusion of the dependence on the macroscopic viscosity. The linear dependence extends over a wider range of concentration when the viscosity term is ignored than when it is included. The curves do approach each other at high concentration, although the slopes are quite different.

Table II
Scaling Parameters α and ν, Entering in Eq 1, Obtained by a Nonlinear Regression Fitting of the Tracer Diffusion Data[a]

	fluorescein		40-kDa dextran		150-kDa dextran		PSS	
matrix M_w	$\alpha \times 10^2$	ν	$\alpha \times 10^2$	ν	$\alpha \times 10^2$	ν	2×10^2	ν
40.6 kDa	0.47	1.05	1.59	0.93	2.11	0.89	2.2	0.92
83 kDa			2.13	0.89	3.12	0.83	1.08	1.12
110 kDa			1.33	1.0	4.28	0.78	3.36	0.86
500 kDa			2.44	0.88	2.4	0.90	4.31	0.91
2 MDa	0.53	1.02	1.7	0.94	7.78	0.72	1.86	1.06

[a] The parameter ν is dimensionless, and α is in units of $(L/g)^{\nu}$.

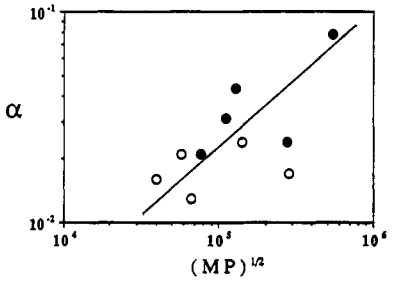

Figure 3. Plot of the scaling parameter α from eq 1 versus the geometric mean of the matrix and probe molecular weights. Probes employed were 40-kDa dextran (○) and 150-kDa dextran (●). The line drawn represents a linear relation between α and $(MP)^{1/2}$ (see eq 12).

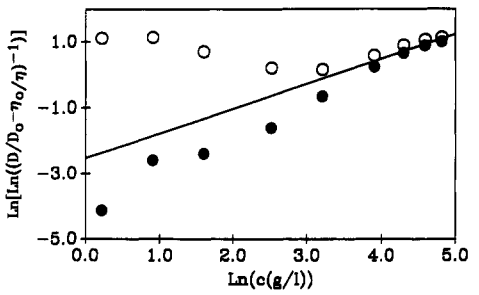

Figure 4. Plot of ln [ln $[(D/D_0 - \eta_0/\eta)^{-1}]$] and ln [ln (D_0/D)] vs ln c (open and closed circles, respectively), where D is the spherical probe diffusion coefficient in a matrix of concentration c, D_0 is the probe diffusion coefficient in water, η_0 is the viscosity of water, and η is the macroscopic viscosity of the dextran solution. The linear regime follows eq 14, and the slope of 0.75 (line drawn) is in agreement with scaling predictions (see text).

The size-dependent impeded diffusion of probes in semidilute polymer solutions is sometimes discussed in terms of deviations from the prediction of the Stokes–Einstein equation (eq 11), where η is the solution viscosity). Values of η calculated from the measured D and known R may deviate substantially from measured values of the macroscopic viscosity.[12,19,20,39-45] Small tracer molecules may be studied to determine the microviscosity of the smaller scale (or the monomer friction),[45] provided there is not a specific association of the tracer and the polymer.[47] We have therefore organized our data for such comparisons by calculating viscosities from the diffusion coefficients measured at different matrix concentrations and the hydrodynamic radii at low concentration. These viscosities are plotted with the measured macroscopic viscosities for the 40-kDa dextran and the 2-MDa dextran in Figure 5. The logarithms of viscosities are plotted to permit comparison over the entire range of concentrations. It is clear that the microscopic viscosity seen by fluorescein is substantially less than the measured macroscopic viscosity over the entire range. Larger probes tend to reflect the macroscopic viscosity at lower matrix concentration and then fall to intermediate values at higher matrix concentration. The dilute-solution values for the macroscopic viscosity permitted a determination of the intrinsic

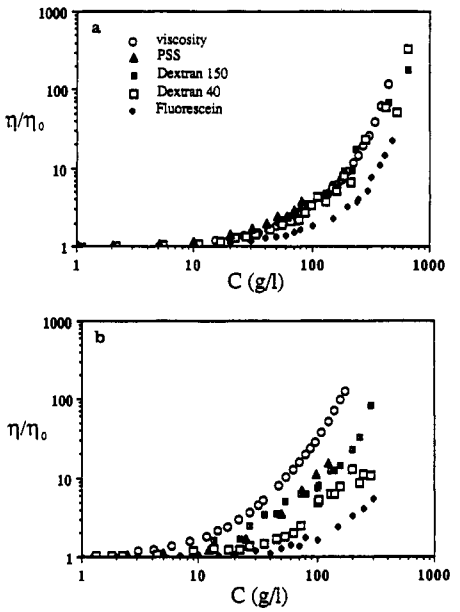

Figure 5. Demonstration of deviation from simple Stokes–Einstein behavior. The logarithm of macroscopic viscosity is plotted as a function of c. Also plotted are viscosities calculated from the diffusion coefficient of various probes using eq 11. (a) Data for the 40-kDa dextran matrix; (b) data for the 150-kDa dextran matrix. Different symbols correspond to different probes as defined in (a).

viscosity of the 40-kDa dextran and the 150-kDa dextran, for which we obtain 0.0127 and 0.0559 L/g, respectively.

Recent reports[48-50] support the idea that translational diffusion in the semidilute regime is due mainly to two mechanisms, namely, a Stokes–Einstein (SE) type of diffusion expressed by eq 11, and reptation. The dominance of any of these processes is determined by the ratio M/P. When this ratio is greater than unity, then the translational diffusion should be well described by eq 11. If $M/P < 1$ then a deviation from the SE equation must be observed, which is attributed to the onset of different mechanisms, including reptation. In Figure 5a we can see that, except for fluorescein with $M = 0.5$ kDa, the D_0/D plots fall almost on the top of the viscosity curve. For PSLS, D_0/D is slightly above, probably due to an extra friction from electrostatic interactions between spheres. For 40-kDa dextran, D_0/D is a little below the viscosity and seems to diverge more at high matrix concentrations. This last feature occurred for 150-kDa dextran as well. Since fluorescein has a much lower molecular weight than the matrix polymers, we expect D_0/D to be a measure of the monomeric (microscopic) viscosity and therefore to be lower than the macroscopic viscosity. Figure 5b shows the case when $M/P < 1$ for all probes. Except at very low concentrations, D_0/D curves fall well below η/η_0 in order of molecular weights. The comparison displayed in Figure 5 clearly suggests a deviation from SE diffusion when $M/P \leq 1$, being larger for lower values of this ratio. From our results such deviations cannot be rationalized in terms of

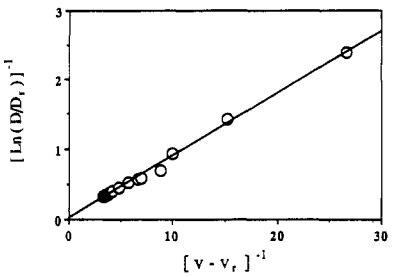

Figure 6. Test of the free-volume theory (eq 18). The linear relationship extends over the concentration regime examined.

an onset of the reptation mechanism alone (see Figure 2).

Finally, we observe that the diffusion of fluorescein depends on matrix polymer concentration but not on P. For polymer–diluent systems the free-volume theory[44,51-54] predicts an exponential decay of the diluent diffusion coefficient with the reciprocal of the system free volume $f(v,T)$; i.e.

$$D = RTA_d \exp(-B_d/f(v,T)) \quad (15)$$

$$f(v,T) = f(0,T) + \beta(T)v \quad (16)$$

and

$$\beta(T) = \gamma(T) - f(0,T) \quad (17)$$

Here v and T are the solvent volume fraction and the temperature, respectively. The different coefficients entering in eqs 15–17 are interpreted as follows: A_d is a factor depending on size and shape of the diluent, B_d is the minimum free volume required by the diluent in order to displace, $f(0,T)$ is the free-volume fraction in the absence of solvent, and $\gamma(T)$ is the free-volume fraction of the solvent. These equations can be rewritten to have the form

$$\frac{1}{\ln(D/D_r)} = \frac{[f(0,T) + \beta(T)v_r]^2}{B_d\beta(T)} \frac{1}{v - v_r} + \frac{f(0,T) + \beta(T)v_r}{B_d} \quad (18)$$

where D_r is a reference value of D corresponding to $v = v_r$. In Figure 6 we plot our data for fluorescein in the form $1/\ln(D/D_r)$ vs $1/(v-v_r)$. A linear relationship is observed even at very low polymer concentrations. D_r is 2.87×10^{-7} cm^2/s and $v_r = 0.7$, corresponding to the highest polymer concentration (480 g/L) we considered. The solvent volume fractions v were calculated from polymer concentrations using the data reported in ref 21.

Recently, Phillies et al.[54a] reported a study of the diffusion of spherical probe particles through aqueous solutions of dextran. They also found that the data were well fit by eq 1. Their values of α and ν are reasonably consistent with ours. However, the systematic decrease of the magnitude of ν and increase of the magnitude of α with P in their studies is not as clear from our data. They observed little dependence of retardation on probe size and little sensitivity of probe diffusion coefficient to matrix polydispersity.

The dextran samples we have employed are the products of commercial fractionation processes and thus may be rather widely polydisperse. Effects of polydispersity have been considered formally,[55-58] with general agreement that they are significant. Callaghan and Pinder[7] studied polydisperse dextran solutions with a range of average molecular weights over a factor of 44 and found that the molecular weight behavior was discernible and reasonable. We have varied matrix molecular weight by a factor of 50 and probe dextran molecular weight by a factor of 3.8. The conclusions we have drawn from these data, particularly regarding the very gradual dependence on molecular weights, must be qualified by the polydispersity issue. Similarly, these dextran chains have short side branches that could affect their diffusion behavior, particularly the molecular weight dependence. We expect this problem to be less important. Dextran is known to contain about 95% α-(1,6) linkages and about 5% α-(1,3) linkages. Previous workers have concluded that the great majority (about 85%) of these side chains are no more than 2 monomer units long, with the very longest no more than 15 monomers.[59] We selected dextran as the experimental system because of the availability of previous results using different techniques and because of its potential importance as a probe of biological media, particularly cell cytoplasm.[60,61] Studies using dextran as a probe of biological media have concluded that it does not experience specific chemical reactions or adsorption and thus is a convenient and nontoxic physical probe of the biological milieu. A better understanding of dextran behavior in semidilute solutions should permit further refinement of the interpretation of those studies.

Supplementary Material Available: Tracer diffusion coefficients of fluorescein-labeled 40-kDa dextran (Table S1), 150-kDa dextran (Table S2), and polystyrene spheres (Table S3) in solutions of dextran of various molecular weights at various mass concentrations; tracer diffusion coefficients of fluorescein in dextran matrices of different molecular weights (Table S4); and viscosity of dextran solutions of molecular weights 40 kDa and 2 MDa at various concentrations (Table S5) (5 pages). Ordering information is given on any current masthead page.

References and Notes

(1) de Gennes, P.-G. *J. Chem. Phys.* **1971**, *55*, 572.
(2) de Gennes, P.-G. *Scaling Concepts in Polymer Physics*; Cornell University Press: Ithaca, NY, 1979.
(3) Leger, L.; Viovy, J. L. *Contemp. Phys.* **1988**, *29*, 579.
(4) Tirrell, M. *Rubber Chem. Technol., Rubber Rev.* **1984**, *57*, 523.
(5) Leger, L.; Hervet, H.; Rondelez, F. *Macromolecules* **1981**, *14*, 1732.
(6) Wesson, J. A.; Noh, I.; Kitano, T.; Yu, H. *Macromolecules* **1981**, *14*, 782.
(7) Callaghan, P. T.; Pinder, D. N. *Macromolecules* **1984**, *17*, 431.
(8) Kim, H.; Chang, T.; Yohanan, J. M.; Wang, L.; Yu, H. *Macromolecules* **1986**, *19*, 2737.
(9) Wheeler, L. M.; Lodge, T. P.; Hanley, B.; Tirrell, M. *Macromolecules* **1987**, *20*, 1120.
(10) Graessley, W. W. *J. Polym. Sci., Polym. Phys. Ed.* **1980**, *18*, 27.
(11) Doi, M.; Edwards, S. F. *J. Chem. Soc., Faraday Trans. 2* **1978**, *47*, 1789, 1802, 1818.
(12) Lodge, T. P.; Markland, P. *Polymer* **1987**, *28*, 1377. (a) Lodge, T. P.; Markland, P.; Wheeler, L. M. *Macromolecules* **1989**, *22*, 3409.
(13) Shull, K. R.; Kramer, E. J.; Hadziioannou, G.; Antonietti, M.; Sillescu, H. *Macromolecules* **1988**, *21*, 2578.
(14) Phillies, G. D. J. *Macromolecules* **1986**, *19*, 2367.
(15) Langevin, D.; Rondelez, F. *Polymer* **1978**, *19*, 875.
(16) Ogston, A. D.; Preston, B. N.; Wells, J. D. *Proc. R. Soc. London A* **1973**, *333*, 297.
(17) Phillies, G. D. J. *Macromolecules* **1987**, *20*, 558.
(18) Chang, T.; Kim, H.; Yu, H. *Macromolecules* **1987**, *20*, 2631.
(19) Brown, W.; Rymden, R. *Macromolecules* **1988**, *21*, 840.
(20) Yam, K. L.; Anderson, D. K.; Buxbaum, R. E. *Science* **1988**, *241*, 330.
(21) *Handbook of Chemistry and Physics*, 62nd ed.; CRC Press: Boca Raton, FL, 1981–1982; p D-206.
(22) Peters, R.; Peters, J.; Tews, K. H.; Bahr, W. *Biochim. Biophys. Acta* **1974**, *367*, 282.
(23) Edidin, M.; Zagyanski, Y.; Lardner, T. J. *Science* **1976**, *191*, 466.
(24) Jacobson, K.; Wu, E.; Poste, G. *Biochim. Biophys. Acta* **1976**, *433*, 215.
(25) Axelrod, D.; Koppel, D. E.; Schlessinger, J.; Elson, E.; Webb, W. *Biophys. J.* **1976**, *16*, 1315.
(26) Lanni, F., Ware, B. R. *Rev. Sci. Instrum.* **1982**, *53*, 905.
(27) Zero, K.; Cyr, D.; Ware, B. R. *J. Chem. Phys.* **1983**, *79*, 3602.

(28) Zero, K.; Ware, B. R. *J. Chem. Phys.* **1984**, *80*, 1610.
(29) Gorti, S.; Ware, B. R. *J. Chem. Phys.* **1985**, *83*, 6449.
(30) Callaghan, P. T.; Pinder, D. N. *Macromolecules* **1983**, *16*, 968.
(31) Callaghan, P. T.; Pinder, D. N. *Macromolecules* **1981**, *14*, 1334.
(32) Haglund, B.-O.; Elisson, M.; Sundelof, L.-O. *Chem. Sc.* **1988**, *28*, 129.
(33) Batchelor, G. K. *Annu. Rev. Fluid Mech.* **1974**, *6*, 227.
(34) Evans, G. T.; James, C. P. *J. Chem. Phys.* **1983**, *79*, 5553.
(35) Venkatesan, M.; Hirtzel, C. S.; Rajagopalan, R. *J. Chem. Phys.* **1985**, *82*, 5685.
(36) Brown, W.; Stilbs, P. *Polymer* **1983**, *24*, 188.
(37) Phillies, G. D. J.; Peczak, P. *Macromolecules* **1988**, *21*, 214.
(38) Cukier, R. I. *Macromolecules* **1984**, *17*, 252.
(39) Yu, T. L.; Reihanian, H.; Jamieson, A. M. *J. Polym. Sci., Polym. Lett. Ed.* **1980**, *18*, 695.
(40) Lin, T.-H.; Phillies, G. D. J. *J. Phys. Chem.* **1982**, *86*, 4073.
(41) Phillies, G. D. J. *Biopolymers* **1985**, *24*, 379.
(42) Ullmann, K.; Ulmann, G. S.; Phillies, G. D. J. *J. Colloid Interface Sci.* **1985**, *105*, 315.
(43) Phillies, G. D. J.; Malone, C.; Ullman, K.; Ullman, G. S.; Rollings, J.; Yu, L.-P. *Macromolecules* **1987**, *20*, 2280.
(44) Huang, W. J.; Frick, T. S.; Landry, M. R.; Lee, J. A.; Lodge, T. P.; Tirrell, M. *AIChE J.* **1987**, *33*, 573.
(45) Pu, Z.; Brown, W. *Macromolecules* **1989**, *22*, 890.
(46) Kim, H.; Chang, T.; Yohanan, J. M.; Wang, L.; Yu, H. *Macromolecules* **1986**, *19*, 2737.
(47) Lee, J. A.; Lodge, T. P. *J. Phys. Chem.* **1987**, *91*, 5546.
(48) Martin, J. E. *Macromolecules* **1986**, *6*, 922.
(49) Numasawa, N.; Kuwamoto, K.; Nose, T. *Macromolecules* **1986**, *19*, 2593.
(50) Brown, W.; Rymden, R. *Macromolecules* **1988**, *21*, 840.
(51) Fujita, H. *Adv. Polym. Sci.* **1961**, *3*, 1.
(52) Vrentas, J. S.; Duda, J. L. *J. Polym. Sci., Polym. Phys. Ed.* **1977**, *15*, 403.
(53) Landry, M. R.; Gu, Q.-J.; Yu, H. *Macromolecules* **1988**, *21*, 1158.
(54) Nemoto, N.; Kojima, T.; Inoue, T.; Kurata, M. *Polym. J.* **1988**, *20*, 875. (a) Phillies, G. D. J.; Gong, J.; Li, L.; Rau, A.; Zhang, K.; Yu, L.-P.; Rollings, J. *J. Phys. Chem.* **1989**, *93*, 6219.
(55) Fleischer, G. *Makromol. Chem., Rapid Commun.* **1985**, *6*, 463.
(56) Bernard, D. A.; Noolandi, J. *Macromolecules* **1983**, *16*, 548.
(57) Lodge, T. P.; Wheeler, L. M.; Hanley, B.; Tirrell, M. *Polym. Bull.* **1986**, *15*, 35.
(58) Choi, K.-S.; Chung, I. J.; Kim, H. Y. *Macromolecules* **1988**, *21*, 3171.
(59) Paine, P. L.; Horowitz, S. B. In *Cell Biology: A Comprehensive Treatise*; Goldstein, L., Prescott, D. M., Eds.; Academic Press: New York, 1980; Vol. 4, pp 299–338.
(60) Lanni, F.; Waggoner, A. S.; Taylor, D. L. *J. Cell Biol.* **1985**, *100*, 1091.
(61) Luby-Phelps, K.; Taylor, D. L.; Lanni, F. *J. Cell Biol.* **1986**, *102*, 2015.

Registry No. Dextran, 9004-54-0; fluorescein, 2321-07-5.